ChemComm

Pressure-induced Dehydrogenative Coupling of Methane to Ethane by Platinum-loaded Gallium Oxide Photocatalyst

Journal:	*ChemComm*
Manuscript ID	CC-COM-03-2020-001730.R1
Article Type:	Communication

COMMUNICATION

Pressure-induced Dehydrogenative Coupling of Methane to Ethane by Platinum-loaded Gallium Oxide Photocatalyst

Received 00th January 20xx,
Accepted 00th January 20xx

DOI: 10.1039/x0xx00000x

Fumiaki Amano,*[ab] Chiho Akamoto,[a] Mizuki Ishimaru,[a] Satoshi Inagaki[b,c] and Hisao Yoshida[d,e]

Pt/Ga_2O_3 exhibited high activity for dehydrogenative coupling of methane into ethane ($2CH_4 \rightarrow C_2H_6 + H_2$) in a fixed-bed flow reactor at 25 °C under 254-nm UV irradiation. The C_2H_6 formation was negligible at CH_4 pressure of 10 kPa, but it was linearly increased with an increase in the pressure to 300 kPa.

CH_4 is an abundant carbon source from natural gas including shale gas, methane hydrate, and renewable biogas.[1] The production of liquid fuels and chemicals from petroleum may be replaced by CH_4.[2, 3] Therefore, catalytic conversion of CH_4 directly into higher hydrocarbons (C_{2+}) is a crucial technology to cope with the concerns of energy security. However, controlling the product selectivity in the direct conversion is a big challenge in catalysis science.[4-6] The most severe issue is the sequential reaction of the desired products, which are more reactive than CH_4, at the high temperatures required to activate the strong C–H bonds (439 kJ mol^{-1}).[7] In this regard, the activation of CH_4 at low temperatures, which may improve the selectivity, is the holy grail of sustainable chemistry.[1-3, 6, 8-12]

Photocatalytic activation of CH_4 proceeds at room temperature despite the endergonic reactions ($\Delta_r G > 0$).[1-3] Many heterogeneous photocatalysts have been investigated for the conversion of CH_4 to yield C_2H_6, which called a non-oxidative coupling of methane (NOCM), $2CH_4 \rightarrow C_2H_6 + H_2$, $\Delta_r G = 68.6$ kJ mol^{-1} at 25 °C.[13-23] The photocatalytic NOCM is induced by highly dispersed metal oxides supported on SiO_2 and zeolites under UV irradiation.[13-21] Semiconductor photocatalysts are also investigated in the absence of oxidant for NOCM.[19, 22] The issue in NOCM is the low quantum efficiency owing to the slow kinetics. Pt-loaded TiO_2–SiO_2:Ga (0.2 g) showed a CH_4 conversion rate of 0.70 μmol h^{-1} with 90% selectivity of C_2H_6, but the apparent quantum efficiency (AQE) was very low (1×10^{-4} % at 350-nm UV irradiation).[23] The CH_4 conversion rate over β-Ga_2O_3 (0.2 g) was 0.05 μmol h^{-1} for NOCM, and the AQE was about 0.01% at wavelengths 220–270 nm.[19]

In this study, we investigated the effect of CH_4 pressure, $P(CH_4)$ on the photocatalytic conversion of CH_4 in the presence of H_2O vapor. We expected that the high concentration of methyl radical ($\bullet CH_3$) promotes the carbon-carbon bond formation to produce C_2H_6. In order to increase the collision frequency of CH_4 on the photocatalyst surface, $P(CH_4)$ was increased from 10 kPa to 300 kPa. First, we screened transition metal oxide photocatalysts loaded with a small amount of Pt cocatalyst, which is the best catalyst minimizing the overpotential necessary to drive H_2 evolution reaction.[24] Second, we focused on the highly active Pt/Ga_2O_3 to prove the concept that high $P(CH_4)$ induce the direct production of C_2H_6.

We performed photocatalytic conversion of CH_4 with H_2O vapor using a fixed-bed flow-type reactor under UV irradiation at 25 °C (Fig. S1, ESI†). Hexachloroplatinate(IV) (H_2PtCl_6, 0.1 wt% as Pt) was loaded on each metal oxide powder by an incipient-wetness impregnation method. The Pt precursor-loaded powder (50 mg) was coated on a glass substrate using water and dried at room temperature. The Pt precursor is quickly reduced to Pt^0 during the initial period of the photocatalytic reaction promoting H_2 evolution.[25] The light source was a 40-W low-pressure mercury lamp (wavelength 254 nm, light intensity 33 or 15 mW cm^{-2}, irradiation area 25 cm^2). The gas mixture of $CH_4/Ar/H_2O$ was continuously supplied to the reactor (volume 5 × 5 × 0.025 cm^3) at a flow rate of 20 mL min^{-1}. The products in the flow system were analyzed by gas chromatography (GC).

We screened 12 oxide powders for photocatalytic H_2 evolution under the stream of 10-kPa CH_4 and 3-kPa H_2O at 1 atm. The physical properties of the oxides are reported in ESI†

[a] Department of Chemical and Environmental Engineering, The University of Kitakyushu, 1-1 Hibikino, Wakamatsu-ku, Kitakyushu, Fukuoka 808-0135, Japan.
[b] Precursory Research for Embryonic Science and Technology (PRESTO), Japan Science and Technology Agency (JST), 4-1-8 Honcho, Kawaguchi, Saitama 332-0012, Japan.
[c] Division of Materials Science and Chemical Engineering, Yokohama National University, 79-5 Tokiwadai, Hodogaya-ku, Yokohama 240-8501, Japan.
[d] Graduate School of Human and Environmental Studies, Kyoto University, Yoshida-nihonmatsu-cho, Sakyo-ku, Kyoto 606-8501, Japan.
[e] Elements Strategy Initiative for Catalysts and Batteries (ESICB), Kyoto University, Kyotodaigaku-Katsura, Nishikyo-ku, Kyoto 615-8520, Japan.

†Electronic Supplementary Information (ESI) available: Experimental details, characterization of the oxide samples, SEM and TEM images of Ga_2O_3, the effect of $P(CH_4)$ on the time courses of product formation rate, TG–DTA, and ESR study. See DOI: 10.1039/x0xx00000x

(Tables S1, S2, Fig. S2–S5). Figure 1 shows the H_2 evolution rate, $r(H_2)$, with 0.1wt% Pt-loaded oxide at 5-min and 65-min photoreaction. Pt/TiO_2 samples (P 25 and ST-01) and Pt/Ta_2O_5 exhibited moderate photocatalytic activity. Pt/ZrO_2 was deactivated in 60 min during the photoreaction. Pt/Ga_2O_3 exhibited the highest activity under 254-nm UV irradiation.[26-29] Since the bandgap of β-Ga_2O_3 was 4.6 eV, the photoexcitation required UV irradiation of wavelengths < 270 nm. The loading of a small amount of Pt cocatalyst significantly enhanced the $r(H_2)$ of Ga_2O_3 (Fig. S6, ESI†).[30] Not only H_2PtCl_6 but also tetraammineplatinum(II) chloride ($Pt(NH_3)_4Cl_2$) could be used for the precursor of Pt cocatalyst (Fig. S7, ESI†). The stability and durability of Pt/Ga_2O_3 were confirmed in a long-term test and repeated reactions (Fig. S8 and S9, ESI†).

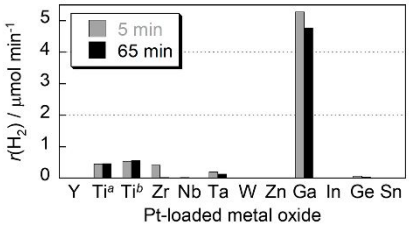

Figure 1. H_2 evolution rate from CH_4 and H_2O with 0.1 wt% Pt-loaded metal oxides under UV light irradiation (254 nm, 33 mW cm^{-2}) for 5 min and 65 min. The metal oxides are Y_2O_3, TiO_2(P 25)[a], TiO_2(ST-01)[b], ZrO_2, Nb_2O_5, Ta_2O_5, WO_3, ZnO, Ga_2O_3, In_2O_3, GeO_2, and SnO_2. Total pressure (P_{total}) =101 kPa. $CH_4/H_2O/Ar$ = 10/3/88.

We selected the highly active TiO_2 and β-Ga_2O_3 photocatalysts for further investigation. Both oxides have been reported to exhibit good performance for photocatalytic H_2 evolution reactions,[25-31] since they have suitable band structures. Figure 2 shows the time course of product formation rates from CH_4 and H_2O vapor with Pt/TiO_2(ST-01) and Pt/Ga_2O_3. ST-01 is an anatase TiO_2 photocatalyst with a large BET specific surface area (S_{BET}). The S_{BET} of ST-01 and β-Ga_2O_3 was 302 m^2 g^{-1} and 10 m^2 g^{-1}. A continuous H_2 evolution (0.21 μmol min^{-1}) was observed for Pt/TiO_2. The O_2 evolution indicates the progress of water splitting ($2H_2O \rightarrow O_2 + 2H_2$) even in the presence of CH_4. The CO_2 generation is explained by photocatalytic steam reforming of methane (photo-SRM, $CH_4 + 2H_2O \rightarrow CO_2 + 4H_2$)[30-32] or oxidation by the evolved O_2 ($CH_4 + 2O_2 \rightarrow CO_2 + 2H_2O$). The ratio of $H_2 : O_2 : CO_2$ was 1 : 0.26 : 0.075 for Pt/TiO_2. In the case of Pt/Ga_2O_3, the evolution of H_2 and O_2 was much higher than that of Pt/TiO_2 but gradually decreased with time. After 3-h photoreaction, the $r(H_2)$ was 1.98 μmol min^{-1}, and the ratio of $H_2 : O_2 : CO_2$ was 1 : 0.30 : 0.065. The CO_2 production was constant during photoreaction. However, there was no production of C_2H_6 and other oxidized products under the condition of $P(CH_4)$ = 10 kPa.‡

The adsorption of CH_4 on the solid surface is not stable since the symmetrical tetrahedral geometry has no dipole moment and small polarizability.[5] Thus, we increased the $P(CH_4)$ to improve the collision frequency of CH_4 molecule on the surface of Pt/Ga_2O_3. Figure 3 shows the time course of the photocatalytic CH_4 conversion using Pt/Ga_2O_3 under high $P(CH_4)$. We have succeeded in the detection of C_2H_6 at $P(CH_4)$ = 98 kPa. We also detected CO formation. At $P(CH_4)$ = 98 kPa, the rate of C_2H_6 production, $r(C_2H_6)$, was slowly increased with time and reached to 0.18 μmol min^{-1} after 3-h photoreaction. The production of CO_2 and C_2H_6 at $P(CH_4)$ = 98 kPa was significantly higher than that at $P(CH_4)$ = 10 kPa (Fig. 2b). The increase in the yield of CO_2 and C_2H_6 indicates that the high $P(CH_4)$ facilitates CH_4 activation and increases the concentration of activated methane species like •CH_3. The O_2 evolution was initially high but diminished with irradiation time. We further increased the total pressure to 3 atm using a back-pressure valve and found that C_2H_6 production was much increased by increasing $P(CH_4)$ from 98 kPa to 300 kPa. The steady-state $r(C_2H_6)$ was 0.58 μmol min^{-1} at 300 kPa. The ratio of $H_2 : CO_2 : CO : C_2H_6$ was 1 : 0.17 : 0.024 : 0.19.§ There was no O_2 evolution at $P(CH_4)$ = 300 kPa.

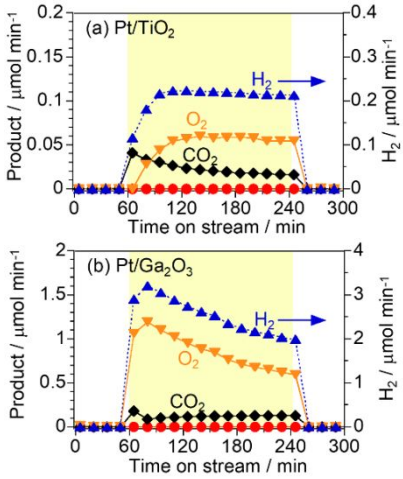

Figure 2. Formation rate of products over (a) Pt/TiO_2(ST-01) and (b) Pt/Ga_2O_3 at P_{total} of 101 kPa ($CH_4/H_2O/Ar$ = 10/3/88). UV light (254 nm, 15 mW cm^{-2}) was irradiated for 3 h (60–240 min time on stream).

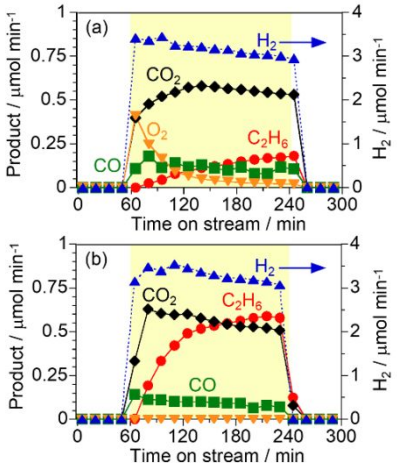

Figure 3. Formation rate of products over Pt/Ga_2O_3 at P_{total} of (a) 101 kPa (CH_4/H_2O = 98/3) and (b) 303 kPa (CH_4/H_2O = 300/3) under 254-nm UV irradiation (15 mW cm^{-2}, 60–240 min time on stream).

Figure 4a shows the effect of $P(CH_4)$ on the formation rate over Pt/Ga_2O_3 after 3-h photoirradiation. The effect of $P(CH_4)$ on the time courses of H_2, C_2H_6, and CO_2 are shown in Fig. S10, ESI†. The C_2H_6 formation was gradually increased with time on stream. The $r(C_2H_6)$ after 3-h photoreaction was monotonically increased with an increase in $P(CH_4)$ from 10 kPa to 300 kPa. In the absence of CH_4, water splitting was induced as proved by

that the H_2/O_2 ratio is 2. The increase in $P(CH_4)$ increased CO_2 production in contrary to the decrease of O_2 production. H_2 production was also increased with $P(CH_4)$ owing to the progress of photo-SRM.[30] However, the production rate of H_2 and CO_2 was almost constant at $P(CH_4) \geq 100$ kPa. The monotonous dependence on $P(CH_4)$ was characteristic of C_2H_6 production.

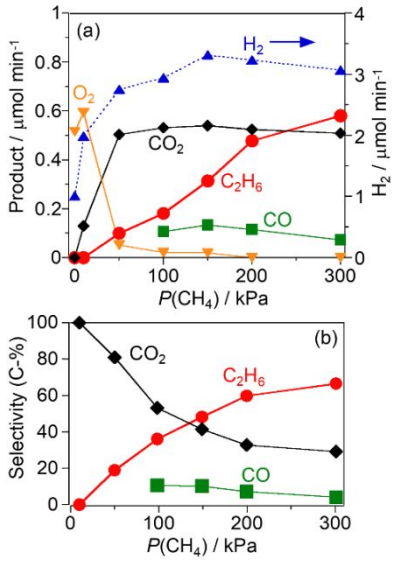

Figure 4. Effect of $P(CH_4)$ on (a) the product formation rate and (b) the carbon-based selectivity in the photocatalytic reaction on Pt/Ga_2O_3. The values were taken from the time course in the flow-type reactor after 3-h photoirradiation. The GC system could not analyze CO when $P(CH_4) < 98$ kPa due to the interference with Ar.

Figure 4b shows the effect of $P(CH_4)$ on the product selectivity on a per carbon basis (C-%). The selectivity of C_2H_6 is defined as the ratio of carbon atoms of the produced C_2H_6 to that of all products containing carbon. The selectivity of C_2H_6 was gradually increased with $P(CH_4)$ and almost saturated at $P(CH_4)$ = 300 kPa. The selectivity of C_2H_6 was 67 C-%, which corresponds to two-thirds of CH_4 molecules becoming ethane and the rest to CO_X. The AQE of the Pt/Ga_2O_3 was calculated from the $r(H_2)$, assuming that one H_2 molecule requires two electrons. The AQE was gradually increased and saturated to be 13% at $P(CH_4) > 100$ kPa (Fig. S11, ESI†). Recently, Li et al. reported H_2 evolution from aqueous H_2O under CH_4 using TiO_2 photocatalysts.[33, 34] The AQE (13%) of the Pt/Ga_2O_3 in this study was higher than that of the gas-solid-liquid Pt/TiO_2 system (4.7% at 254-nm irradiation with C_2H_6 selectivity of 62 C-%). The high efficiency is provided by the intrinsic activity of Ga_2O_3, the loading of Pt cocatalyst, and the photocatalytic reaction conditions. Noted that the error in material balance was less than 10%, assuming that C_2H_6, O_2, CO, and CO_2 come from dehydrogenative reactions (Fig. S12, ESI†). The small amount of missing was related to the formation of carbon species on the photocatalyst surface, which was confirmed by thermogravimetry–differential thermal analysis (TG–DTA, Fig. S13, ESI†).

The rate of CH_4 conversion per photocatalyst weight was often reported to compare the performance of the photocatalytic system. However, this evaluation is not accurate because the reaction rate is not always proportional to the photocatalyst weight.[35] When we tentatively calculated it from the formation rate of carbon-contained products, the CH_4 conversion rate was 2090 μmol g^{-1} h^{-1} (1.74 μmol min^{-1} over 50-mg Pt/Ga_2O_3), which was much higher than the reported values.[23]

We measured electron spin resonance (ESR) spectra of the Ga_2O_3 powder at −196 °C. The Ga_2O_3 evacuated at room temperature for 30 min generated a sharp signal at around 326 mT (g = 2.003) by UV irradiation (Fig. S14, ESI†). The presence of CH_4 (10 kPa) changed the intensity and the shape of the ESR signal. The interaction with CH_4 suggests that the radical species are related to the photogenerated holes trapped in the surface states (h_{tr}^+). The UV-induced signal was not observed for the dehydrated Ga_2O_3, which was pre-evacuated at 200 °C to remove the adsorbed water species (Fig. S15, ESI†). Therefore, the hole trapping site interacts with the hydroxyl group or the water molecules adsorbed on the surface. The h^+ trapped in the surface hydroxyl group ($h_{tr(OH)}^+$) would be like a surface hydroxyl radical ($\bullet OH_S$). We could not detect the ESR signal of $\bullet CH_3$ in the gas phase,[36] but the C_2H_6 is considered to form via the coupling of $\bullet CH_3$ on the surface. The proposed reaction mechanism can be expressed as follows.

$$Ga_2O_3 + h\upsilon \rightarrow e^- + h_{tr(OH)}^+ \#(1)$$

$$CH_4 + h_{tr(OH)}^+ \xrightarrow{k} \bullet CH_3 + H^+ \#(2)\#$$

$$\bullet CH_3 + \bullet CH_3 \rightarrow C_2H_6 \#(3)$$

$$2H^+ + 2e^- \xrightarrow{\text{Pt cocatalyst}} H_2 \#(4)$$

The valence band maximum of Ga_2O_3 (Figure S4, ESI†) can thermodynamically induce one-electron oxidation of CH_4 ($CH_4 \rightarrow \bullet CH_3 + H^+ + e^-$, E = 2.06 V vs. SHE).[9] When the oxidation of CH_4 by the trapped $h_{tr(OH)}^+$ expressed by equation (2) is the rate-determining step, the $r(C_2H_6)$ is proportional to the $P(CH_4)$ and the concentration of $h_{tr(OH)}^+$.

$$r(C^2H^6) = 0.5k[h_{tr(OH)}^+]P(CH^4)\#(5)$$

As shown in Figure 4a, the C_2H_6 formation over Pt/Ga_2O_3 was monotonically increased with an increase in $P(CH_4)$. Figure 5 shows the kinetic analysis of the dependence of $r(C_2H_6)$ on $P(CH_4)$. The reaction order of C_2H_6 formation was 1.04 with respect to the CH_4 concentration. The first-order kinetics is consistent with the rate law derived from the proposed reaction mechanism (Eq. 5). The coupling between $\bullet CH_3$ molecules should be much faster than the C–H bond cleavage. If $\bullet CH_3$ does not react with another $\bullet CH_3$ due to the low concentration, the $h_{tr(OH)}^+$ promotes further overoxidation. The $r(CO_2)$ was saturated at least $P(CH_4)$ = 50 kPa (Figure 4a), suggesting that the rate-determining step for CO_2 generation includes the reaction of the adsorbed C_1 species. The $r(H_2)$ was also saturated at high $P(CH_4)$, implying that the rate-determining step of H_2 evolution is related to the C–H bond cleavage of the adsorbed C_1 species. We confirmed that the product formations were dependent on the light intensity, but $r(C_2H_6)$ was saturated at high light intensity (Fig. S16, ESI†). This suggests

that high photon flux accelerates overoxidation of CH_4 rather than selective oxidation to C_2H_6. The role of Pt was found to promote proton reduction since the $r(H_2)$ was significantly increased by the loading of a small amount of Pt (Fig. S6 and S7, ESI†). The formation of Pt metal particles was confirmed for the Pt/Ga_2O_3 after photocatalytic reaction by UV-Visible spectroscopy (Fig. S17, ESI†). Transmission electron microscopy revealed that Pt nanoparticles were highly dispersed on the Ga_2O_3 surface, and the particle size is less than at least 2 nm (Fig. S18, ESI†).

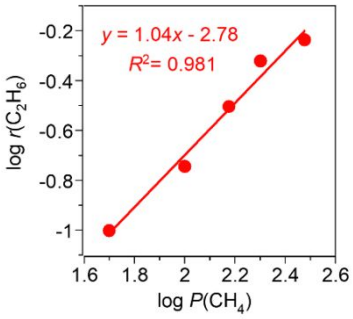

Figure 5. Relationship between $P(CH_4)$ and the C_2H_6 formation rate over Pt/Ga_2O_3 under 254-nm UV irradiation (15 mW cm^{-2}) at $P(H_2O)$ = 3 kPa.

In conclusion, we have found that dehydrogenative CH_4 coupling by Pt/Ga_2O_3 photocatalyst was induced under high $P(CH_4)$ in the presence of H_2O vapor. C_2H_6 formation was not observed at $P(CH_4)$ = 10 kPa, but proportionally increased with $P(CH_4)$. The C_2H_6 formation rate was significantly high (35 µmol h^{-1} on 50-mg Pt/Ga_2O_3) at $P(CH_4)$ = 300 kPa. The C_2H_6 selectivity was 67 C-% when the CH_4 conversion rate was 104 µmol h^{-1}. The AQE of Pt/Ga_2O_3 was 13% at 254-nm irradiation. The interaction of CH_4 on the photocatalyst surface was critical not only to the CH_4 conversion but also to the product selectivity in the photocatalytic system at room temperature.

This work was supported by the Japan Science and Technology Agency (JST), Precursory Research for Embryonic Science and Technology (PRESTO), grant numbers JPMJPR15S1, JPMJPR16S2, and JPMJPR18T1.

Notes and references

‡ We could not analyze a small amount of CO in the presence of Ar carrier due to the interference in GC analysis.

§ The formation of methanol and propane was not detected by GC in this study.

1. H. Song, X. Meng, Z. J. Wang, H. Liu and J. Ye, *Joule*, 2019, **3**, 1606-1636.
2. J. Baltrusaitis, I. Jansen and J. D. Schuttlefield Christus, *Catal. Sci. Technolog.*, 2014, **4**, 2397-2411.
3. K. Shimura and H. Yoshida, *Catal. Surv. Asia*, 2014, **18**, 24-33.
4. X. Guo, G. Fang, G. Li, H. Ma, H. Fan, L. Yu, C. Ma, X. Wu, D. Deng, M. Wei, D. Tan, R. Si, S. Zhang, J. Li, L. Sun, Z. Tang, X. Pan and X. Bao, *Science*, 2014, **344**, 616-619.
5. P. Schwach, X. Pan and X. Bao, *Chem. Rev.*, 2017, **117**, 8497-8520.
6. K. Ohkubo and K. Hirose, *Angew. Chem. Int. Ed.*, 2018, **57**, 2126-2129.
7. Y.-R. Luo, *Comprehensive Handbook of Chemical Bond Energies*, CRC Press, Boca Raton, 2007.
8. A. Hu, J. J. Guo, H. Pan and Z. Zuo, *Science*, 2018, **361**, 668-672.
9. F. Amano, A. Shintani, K. Tsurui, H. Mukohara, T. Ohno and S. Takenaka, *ACS Energy Lett.*, 2019, **4**, 502-507.
10. A. Sato, S. Ogo, K. Kamata, Y. Takeno, T. Yabe, T. Yamamoto, S. Matsumura, M. Hara and Y. Sekine, *Chem. Commun.*, 2019, **55**, 4019-4022.
11. Q. Han, A. Tanaka, M. Matsumoto, A. Endo, Y. Kubota and S. Inagaki, *RSC Adv.*, 2019, **9**, 34793-34803.
12. N. Levin, J. Lengyel, J. F. Eckhard, M. Tschurl and U. Heiz, *J. Am. Chem. Soc.*, 2020, **142**, 5862-5869.
13. Y. Kato, H. Yoshida and T. Hattori, *Chem. Commun.*, 1998, DOI: 10.1039/a806825i, 2389-2390.
14. H. Yoshida, N. Matsushita, Y. Kato and T. Hattori, *J Phys Chem B*, 2003, **107**, 8355-8362.
15. H. Yoshida, M. G. Chaskar, Y. Kato and T. Hattori, *J. Photochem. Photobiol. A Chem.*, 2003, **160**, 47-53.
16. L. Yuliati, T. Hattori and H. Yoshida, *Phys. Chem. Chem. Phys.*, 2005, **7**, 195-201.
17. L. Yuliati, T. Hamajima, T. Hattori and H. Yoshida, *J. Phys. Chem. C*, 2008, **112**, 7223-7232.
18. L. Yuliati and H. Yoshida, *Chem. Soc. Rev.*, 2008, **37**, 1592-1602.
19. L. Yuliati, T. Hattori, H. Itoh and H. Yoshida, *J. Catal.*, 2008, **257**, 396-402.
20. L. Li, G. D. Li, C. Yan, X. Y. Mu, X. L. Pan, X. X. Zou, K. X. Wang and J. S. Chen, *Angew. Chem. Int. Ed.*, 2011, **50**, 8299-8303.
21. L. Li, Y. Y. Cai, G. D. Li, X. Y. Mu, K. X. Wang and J. S. Chen, *Angew. Chem. Int. Ed.*, 2012, **51**, 4702-4706.
22. L. Meng, Z. Chen, Z. Ma, S. He, Y. Hou, H. H. Li, R. Yuan, X. H. Huang, X. Wang, X. Wang and J. Long, *Energy Environ. Sci.*, 2018, **11**, 294-298.
23. S. Wu, X. Tan, J. Lei, H. Chen, L. Wang and J. Zhang, *J. Am. Chem. Soc.*, 2019, **141**, 6592-6600.
24. Z. W. Seh, J. Kibsgaard, C. F. Dickens, I. Chorkendorff, J. K. Nørskov and T. F. Jaramillo, *Science*, 2017, **355**, eaad4998.
25. F. Amano, O. O. Prieto-Mahaney, Y. Terada, T. Yasumoto, T. Shibayama and B. Ohtani, *Chem. Mater.*, 2009, **21**, 2601-2603.
26. T. Yanagida, Y. Sakata and H. Imamura, *Chem. Lett.*, 2004, **33**, 726-727.
27. L. Yuliati, H. Itoh and H. Yoshida, *Chem. Phys. Lett.*, 2008, **452**, 178-182.
28. H. Tsuneoka, K. Teramura, T. Shishido and T. Tanaka, *J. Phys. Chem. C*, 2010, **114**, 8892-8898.
29. Y. Sakata, Y. Matsuda, T. Nakagawa, R. Yasunaga, H. Imamura and K. Teramura, *ChemSusChem*, 2011, **4**, 181-184.
30. K. Shimura, T. Yoshida and H. Yoshida, *J. Phys. Chem. C*, 2010, **114**, 11466-11474.
31. H. Yoshida, K. Hirao, J. I. Nishimoto, K. Shimura, S. Kato, H. Itoh and T. Hattori, *J. Phys. Chem. C*, 2008, **112**, 5542-5551.
32. K. Shimura and H. Yoshida, *Energy Environ. Sci.*, 2010, **3**, 615-617.
33. L. Yu, Y. Shao and D. Li, *Appl. Catal. B Environ.*, 2017, **204**, 216-223.
34. L. Yu and D. Li, *Catal. Sci. Technolog.*, 2017, **7**, 635-640.
35. H. Yoshida, S. Mizuba and A. Yamamoto, *Catal Today*, 2019, **334**, 30-36.
36. D. J. Driscoll, W. Martir, J. X. Wang and J. H. Lunsford, *J. Am. Chem. Soc.*, 1985, **107**, 58-63.

Table of contents entry

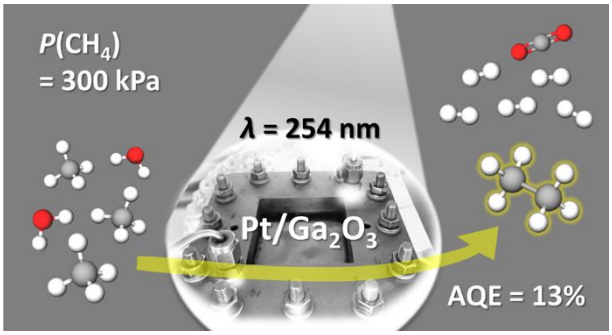

Pt/Ga_2O_3 induced photocatalytic dehydrogenative coupling of CH_4 to yield C_2H_6 under high CH_4 pressure.